VI. MICROWAVE ELECTRONICS*

Prof. L. D. Smullin	A. Bers	B. A. Highstrete
Prof. H. A. Haus	R. M. Bevensee	A. J. Lichtenberg
Prof. S. Saito (Visiting Fellow)	H. W. Fock†	A. H. Czarapata
	C. Fried	

A. THEORY OF COUPLING OF MODES IN LOSSLESS UNIFORM CYLINDRICAL SYSTEMS

Pierce (1) introduced the theory of mode coupling in order to analyze the interaction between modes pertaining to two different propagating systems. The potentialities of the theory of mode coupling were impeded by the fact that the identification of the modes and the evaluation of the coupling coefficients in specific cases were not clear. The work reported here establishes a mathematical method for the identification of modes and for the evaluation of the coupling coefficients. The work is applicable to coupled slow-wave systems. The method is based on recognizing that a coupling-of-modes formalism is intrinsically an expansion of fields in terms of the modes of two systems.

For purposes of illustration, we shall have two examples in mind when developing the general formalism. The structure of Fig. VI-1a consists of two cylindrical reactive walls of circular cross section. These walls may not be concentric, a fact which would make difficult a direct computation (by methods other than mode-coupling). The other example (Fig. VI-1b) is a traveling-wave tube consisting of a longitudinal, cylindrical electron beam in a slow-wave structure (such as a helix in a conducting tube). The beam is confined to longitudinal motion by an infinite magnetic-focusing field. Common to both examples is the fact that they are composed of two subsystems, as shown in Fig. VI-2a and b. Each of the subsystems is a structure with modes of its own.

The field of the entire system can be expanded in terms of the modes of any one of the two subsystems (2, 3). If a slow-wave solution is sought that has large energy densities near both subsystems (for example, near the electron beam, and near the helix of Fig. VI-1b) more rapid convergence of the resulting series can be obtained if the expansion is made in terms of the modes of both subsystems. Denote by $\overline{e_n}(x, y)$ and $\overline{h_n}(x, y)$ the transverse vector dependence of the E and H fields of the n^{th} propagating mode of the inner system at a particular frequency, with the outer system removed. The propagation constant of the mode is γ_n, $[\mathrm{Re}(\gamma_n) = 0]$. Denote the corresponding quantities of the ν^{th} exponential (cutoff) mode of the inner system by the same symbols with the subscript ν, $[\mathrm{Re}(\gamma_\nu) \neq 0]$. We shall also allow for a

*This research was supported in part by Purchase Order DDL-B187 with Lincoln Laboratory, which is supported by the Department of the Army, the Department of the Navy, and the Department of the Air Force under Contract AF19(122)-458 with M.I.T.

†From Raytheon Manufacturing Company.

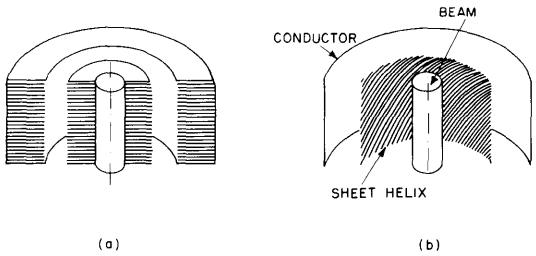

Fig. VI-1. (a) Slow-wave structure. (b) Traveling-wave tube.

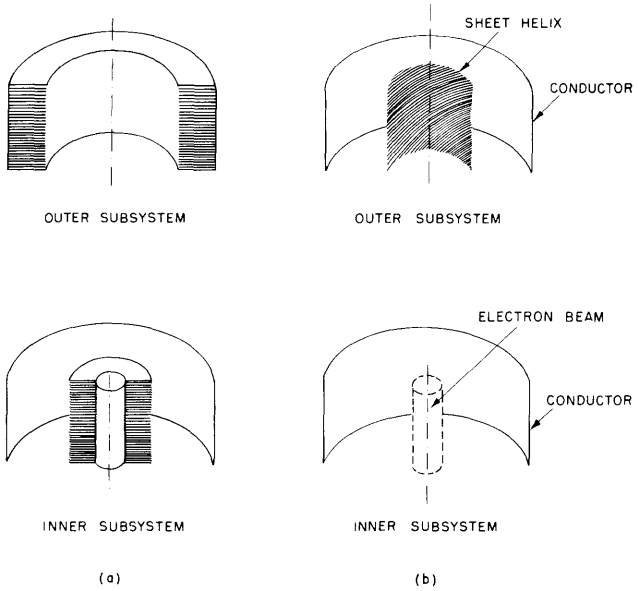

Fig. VI-2. (a) Subsystems of Fig. VI-1a. (b) Subsystems of Fig. VI-1b.

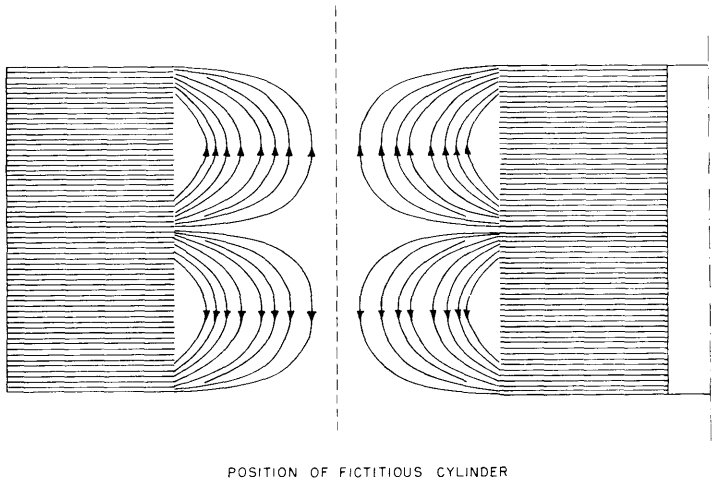

Fig. VI-3. The field of a slow wave.

convection-current density j_n (or j_ν) to be associated with the mode of the inner system. Further, denote the transverse dependences of the fields of the m^{th} propagating mode of the outer system by $\bar{E}_m(x, y)$ and $\bar{H}_m(x, y)$, its propagation constant by Γ_m, $[\mathrm{Re}(\Gamma_m) = 0]$. The exponential (cutoff) modes of the outer system will be distinguished by the subscript μ.

Let us now look for a mode of the combined system with a z-dependence of the form $\exp(-\Gamma z)$. We decompose the entire field $\bar{E}(x, y, z)$ and $\bar{H}(x, y, z)$ into two parts by a fictitious cylinder, placed between the inner and outer structure. As an example, we show a sketch (Fig. VI-3) of the field of the cylindrically symmetric slow mode of the structure of Fig. VI-1a. The cylinder is shown in the region of weak field. The entire field is split into two parts:

$$\bar{E}_i(x, y, z) = \bar{E}(x, y, z), \quad \text{inside cylinder}$$

$$= 0 \quad , \quad \text{outside cylinder}$$

$$\bar{E}_o(x, y, z) = \bar{E}(x, y, z), \quad \text{outside cylinder}$$

$$= 0 \quad , \quad \text{inside cylinder}$$

and correspondingly for the H-field.

The fields $\bar{E}_i$ and $\bar{H}_i$ may be thought of as being produced by magnetic and electric surface currents, $\bar{k}^{(m)}$ and $\bar{k}^{(e)}$ in the surface of the cylinder:

$$\bar{k}^{(m)} = +\bar{n} \times \bar{E} \qquad \bar{k}^{(e)} = -\bar{n} \times \bar{H} \tag{1}$$

where $\bar{n}$ is the unit vector normal on the cylinder directed inward, and $\bar{E}$ and $\bar{H}$ are the actual fields on the surface of the fictitious cylinder.

Correspondingly, the fields $\bar{E}_o$ and $\bar{H}_o$ may be thought of as being produced by surface currents $\bar{K}^{(e)}$ and $\bar{K}^{(m)}$:

$$\bar{K}^{(e)} = -\bar{k}^{(e)} \qquad \bar{K}^{(m)} = -\bar{k}^{(m)} \tag{2}$$

An expansion of $\bar{E}_i$ and $\bar{H}_i$ in terms of the modes $\bar{e}_n$ and $\bar{h}_n$ is now equivalent to the evaluation of the fields in the inner structure that are produced by a prescribed current distribution. Assuming the set of modes $\bar{e}_n$, $\bar{h}_n$ to be complete, we obtain

$$\bar{E}_i(x, y, z) = e^{-\Gamma z} \sum_{n, \nu} a_k \bar{e}_k$$

$$\bar{H}_i(x, y, z) = e^{-\Gamma z} \sum_{n, \nu} a_k \bar{h}_k \tag{3}$$

$$\bar{J}_i(x, y, z) = e^{-\Gamma z} \sum_{n, \nu} a_k \bar{j}_k$$

(It can be shown that the set is complete in the case of the slow-wave structure of Fig. VI-1a.) Similarly, for the expansion of the outer field, $\overline{E}_o$, $\overline{H}_o$, we obtain

$$\overline{E}_o(x, y, z) = e^{-\Gamma z} \sum_{m, \mu} A_k \overline{E}_k$$

$$\overline{H}_o(x, y, z) = e^{-\Gamma z} \sum_{m, \mu} A_k \overline{H}_k \tag{4}$$

The coefficients a_k can be found in terms of the fictitious driving currents of the inner system, $\overline{k}^{(m)}$ and $\overline{k}^{(e)}$ on the cylinder, by means of an extension of Kino's general orthogonality relations (3). Similarly, we can obtain the amplitudes A_k of the modes of the outer system in terms of the currents $\overline{K}^{(m)}$ and $\overline{K}^{(e)}$. Finally, we express the surface currents $\overline{k}^{(m)}$ and $\overline{k}^{(e)}$ in terms of the field expansions, Eqs. 4, the surface currents $\overline{K}^{(m)}$ and $\overline{K}^{(e)}$ in terms of the field expressions, Eqs. 3. The result is a set of coupling equations:

$$\Gamma a_j = \gamma_j a_j + \sum_{m, \mu} c_{jk} A_k$$

$$\Gamma A_j = \Gamma_j A_j + \sum_{n, \nu} C_{jk} a_k \tag{5}$$

where

$$c_{nk} = \frac{1}{4p_n} \oint \left(\overline{E}_k \times \overline{h}_n^* + \overline{e}_n^* \times \overline{H}_k \right) \cdot \overline{n} \, ds$$

$$c_{\nu k} = \frac{1}{4p_\nu} \oint \left(\overline{E}_k \times \overline{h}_{-\nu}^* + \overline{e}_{-\nu}^* \times \overline{H}_k \right) \cdot \overline{n} \, ds$$

$$C_{mk} = -\frac{1}{4P_m} \oint \left(\overline{e}_k \times \overline{H}_m^* + \overline{E}_m^* \times \overline{h}_k \right) \cdot \overline{n} \, ds \tag{6}$$

$$C_{\mu k} = -\frac{1}{4P_\mu} \oint \left(\overline{e}_k \times \overline{H}_{-\mu}^* + \overline{E}_{-\mu}^* \times \overline{h}_k \right) \cdot \overline{n} \, ds$$

The subscripts n and ν, m and μ, stand for propagating and exponentially growing or

decaying (cutoff) modes, respectively. The mode with a complex-conjugate propagation constant to that of the ν^{th} mode is denoted by $-\nu$. The contour integrals refer to an integration over the contour of the fictitious cylinder. P_m is the power associated with the m^{th} propagating mode of the outer system, when $|A_m| = 1$; p_n denotes the corresponding quantity for the inner structure. This power includes the well-known kinetic power of an electron beam if the system contains a beam. The value p_ν is associated with the cross power of the cutoff modes. In the absence of an electron beam,

$$p_\nu = \frac{1}{4} \int \bar{i}_z \cdot \left(\bar{e}_{+\nu} \times \bar{h}^*_{-\nu} + \bar{e}^*_{-\nu} \times \bar{h}_{+\nu} \right) ds = p^*_{-\nu}$$

where $\bar{i}_z$ is the unit vector in the z-direction, and the integral is carried over the cross section of the inner system. A corresponding relation holds for P_μ.

Equations 5 can be interpreted as coupled transmission line equations, if we note that multiplication by Γ means differentiation with regard to z. These transmission line equations have to fulfill certain power-conservation requirements. Indeed, from the way the problem has been formulated, it must be expected that the power, computed as the sum of the powers in the individual modes of the subsystems, integrated over the cross sections of the subsystems, must be independent of distance. It can be easily checked, with the aid of Eq. 6, that

$$C_{mn} = -\frac{p_n}{P_m} c^*_{nm}$$

$$C_{m\nu} = -\frac{p_{-\nu}}{P_m} c^*_{-\nu m}$$

$$C_{\mu n} = -\frac{p_n}{P_\mu} c^*_{n-\mu}$$

$$C_{\mu\nu} = -\frac{p_{-\nu}}{P_\mu} c^*_{-\nu-\mu}$$

These conditions are necessary and sufficient for the fulfillment of power conservation.

Finally, let us look briefly into an application of the above-mentioned formalism, a traveling-wave tube with a thick beam, as in Fig. VI-1b. We assume that the space-charge modes are large and that the slow circuit wave is synchronous with the slow wave of the dominant space-charge mode. Using Maxwell's equations and Gauss' theorem, we may transform the coupling coefficient C_{mn} that corresponds to these two modes into a different form. The current in the beam is assumed to be entirely z-directed ($\bar{j}_n = \bar{i}_z j_n$). We obtain

$$C_{mn} = -\frac{1}{4P_m}\left[\oint \bar{e}_n \times \bar{H}_m^* \cdot \bar{n}\, ds + \oint \bar{E}_m^* \times \bar{h}_n \cdot \bar{n}\, ds\right]$$

$$= \frac{1}{4P_m}\int \left[E_{mz}^* j_n - \left(\Gamma_m^* + \Gamma_n\right)\left(\bar{e}_n \times \bar{H}_m^* + \bar{E}_m^* \times \bar{h}_n\right) \cdot \bar{i}_z\right] da \approx \frac{1}{4P_m}\int E_{mz}^* j_n\, da$$

where the integrals are extended over the interior of the fictitious cylinder. Since $j_n = 0$ everywhere except within the electron beam, the last integral extends only over the cross section of the electron beam. The last expression is an approximation that is valid at small values of coupling, when the electromagnetic power in the beam is much smaller than the kinetic power.

If the coupling among all other modes is neglected, the set of coupling equations (Eqs. 5) yields a quadratic equation for the propagation constants. Comparison with Pierce's solutions for large QC then leads to the conclusion that Pierce's K, which describes the coupling of the circuit wave to the slow, dominant, space-charge wave of a thick beam, has to be defined as

$$K = \frac{1}{2\beta^2 P_m}\,\frac{\left|\int E_{zm}^* j_n\, da\right|^2}{a\int |j_n|^2\, da}$$

where j_n is the distribution of the current in the dominant space-charge wave, and the integration is carried over the beam cross section; P_m is the electromagnetic power in the slow wave that produces the field distribution E_{zm} in the beam; and a is the area of the beam cross section.

H. A. Haus

References

1. J. R. Pierce, Coupling of modes of propagation, J. Appl. Phys. 25, 179-183 (1954).
2. J. R. Pierce, Theory of the beam-type traveling-wave tube, Proc. IRE 35, 111-123 (1947).
3. G. S. Kino, Normal mode theory of perturbed transmission systems, Technical Report 84, Stanford University, May 2, 1955.

B. MULTICAVITY KLYSTRONS*

Analog computer programming of multicavity klystrons (Quarterly Progress Report, Jan. 15, 1957, p. 40) continues. Variations in the gain per stage, cavity permutations,

*This work was supported in part by the Office of Naval Research under Contract Nonr 1841(05).

and new detunings are being investigated. A new program is being initiated with the aim of exploring the nature of current growth in multicavity klystrons and its relation to the efficiency of such tubes.

A. Bers

C. ELECTROLYTIC TANK STUDIES*

A study of the electrolytic tank has been undertaken in order to be able, eventually, to plot electron trajectories with the aid of an analog computer. For such computations, it is necessary to measure the vector electric field at the position of the electrons, as simulated in a tank.

A small electrolytic tank is being used to test various probes and the necessary isolation circuitry. The probe unit now being used consists of a pair of cathode followers for each x and y input. (See Fig. VI-4.) Capacitors are used on each cathode follower to reduce quadrature variations that result from the changing positions of the probe. The differential output of the cathode followers, which is the gradient between the two probes, is obtained through a transformer.

Depth sensitivity of the probe was reduced by coating the probes with insulation within a small distance of the tips. With the coated probes a constant conducting area is always exposed to the electrolyte, even though the probes vary in depth below the surface. Also, by insulating the probes to some depth below the surface, the distortion caused by the rising meniscus is reduced. The coated probes have practically

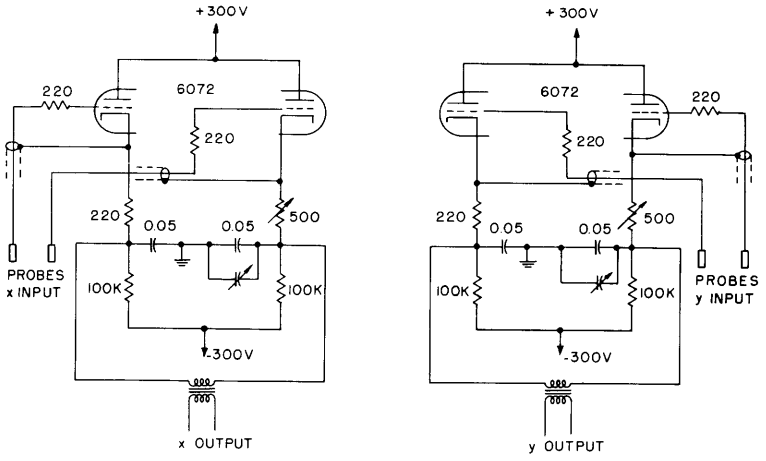

Fig. VI-4. Cathode-follower isolation amplifier.

*This work was supported in part by the Office of Naval Research under Contract Nonr 1841(05).

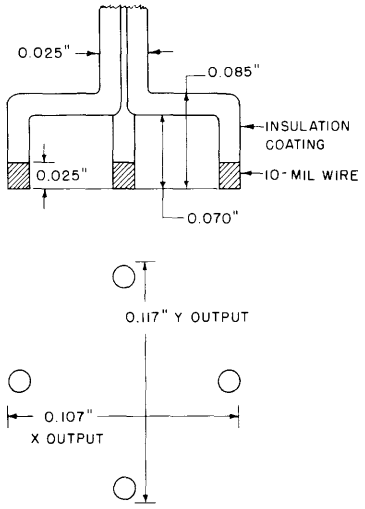

Fig. VI-5. Design for reducing field distortion by meniscus.

eliminated the phase-shift variation which accompanies the variation of the depth of the probes. Coating the probes also increases the equivalent source impedance, but not excessively.

Several probe designs were investigated. (See Fig. VI-5.) The probe design in which the four individual probes enter the water together and then branch out is several times less sensitive to depth than the one in which each probe enters the water individually. The meniscus effect in the design which has each probe entering separately tends to draw the water up between the probes and thus causes field distortion.

In either design, variations of the output of the probe approach 1 per cent of the maximum output signal, as the probe is moved around in the uniform field of the tank. These variations occur principally in the vicinity of the electrodes, within approximately 1 cm, and are essentially attributable to the distortion of the field by the meniscus on the electrode and to polarization effects. The meniscus effects near the electrodes were considerably reduced by placing the top of the electrode flush with the surface, or even submerging it slightly below the surface.

G. H. Pfersch, Jr.

[Mr. Pfersch is a member of the Dynamic Analysis and Control Laboratory, M.I.T.]

D. SEVEN-CAVITY, STAGGER-TUNED, HOLLOW-BEAM KLYSTRON*

1. Introduction

In the Quarterly Progress Report of January 15, 1957, page 46, the analysis of a seven-cavity, stagger-tuned klystron indicated that we might achieve a small signal bandwidth of approximately 5 times that of the intermediate cavities. Thus if these cavities had loaded Q's of $Q_L = 100$, the entire tube would have a 5 per cent bandwidth. If high-perveance beams can be used, the Q_L of the intermediate cavities can be reduced to 30 or 40, without an excessive sacrifice in gain, so that over-all bandwidths of approximately 15 per cent may be achieved. Table VI-I illustrates the basic electrical

*This work was supported in part by the Office of Naval Research under Contract Nonr 1841(05).

Table VI-I. Design Data for Multicavity Klystron.

Frequency	f_o = 1200 mc	
Wavelength	λ_o = 25 m	
Pulse beam power	$P_o = 5 \times 10^6$ watts	
	Solid Beam	Hollow Beam
Perveance	$K = 2 \times 10^{-6}$	$K = 10^{-5}$
Pulse voltage	V_o = 87 kv	V_o = 48 kv
Pulse current	I_o = 57.3 amp	I_o = 104 amp
Fraction of light velocity	$v_o/c = 0.59$	$v_o/c = 0.438$
Relative beam radius	$\gamma b = 0.56$	$\gamma b = 1.35$
Relative gap radius	$\gamma a = 0.8$	$\gamma a = 1.5$
Beam radius	b = 1.64 cm	b = 2.6 cm
Beam thickness		t = 0.15b = 0.39 cm
Gap diameter	a = 2.35 cm	a = 2.9 cm
Current density	$J_o = 6.75$ a/cm^2	$J_o = 17.8$ a/cm^2
Relative plasma frequency	$\omega_p/\omega = 0.369$	$\omega_p/\omega = 0.68$
Plasma reduction factor	$\omega_q/\omega_p = 0.38$	$\omega_q/\omega_p = 0.18$
Relative reduced plasma frequency	$\omega_q/\omega = 0.14$	$\omega_q/\omega = 0.12$
Relative plasma wavelength	$\lambda_q/\lambda = 4.15$	$\lambda_q/\lambda = 3.53$
Plasma wavelength	λ_q = 103.5 cm = 40.8 inches	λ_q = 88.4 cm = 34.8 inches
Seven-cavity interaction length ($\lambda_q/4$ spacing between cavities)	L = 59 inches	L = 52.2 inches
DC-magnet field	B_o = 530 gauss	B_o = 700 gauss

design of such a tube, comparing a solid beam of perveance $K = 2 \times 10^{-6}$, and a hollow beam of perveance $K = 10^{-5}$.

The tube is being designed for operation at approximately 1200 mc, since this allows us to use a hollow beam of perveance $K = 10^{-5}$ derived from a confined flow parallel gun. (We decided not to compound problems by requiring a convergent hollow-beam gun. If such a gun were available, we could operate at higher frequencies – 3000 mc – without excessive cathode current-density requirements.)

The basic components of such a tube are a hollow-beam gun, hollow-beam focusing magnets, low-Q intermediate cavities, a lower-Q input cavity, and a very low-Q output cavity.

L. D. Smullin, A. Bers, H. W. Fock, A. H. Czarapata

2. Hollow-Beam Gun

The design of a parallel-flow gun of perveance K = 10^{-5} was completed. The beam thickness is 0.124 inch; its outer radius is 1.236 inches. The cathode consists of a nickel annulus and heater-coil chamber mounted on a quartz disk. The inner and outer cathode electrodes are each bolted to a stainless steel ring with three studs. The ring, in turn, is supported from the quartz disk by three lava spacers. This entire assembly is insulated from the stainless steel casing by a ceramic spacer. A mild steel plate at the rear of the gun maintains a parallel magnetic field in the cathode region. The gun will be operated with the cathode at -40 kv and the casing at ground potential. (See Fig. VI-6.)

A. H. Czarapata

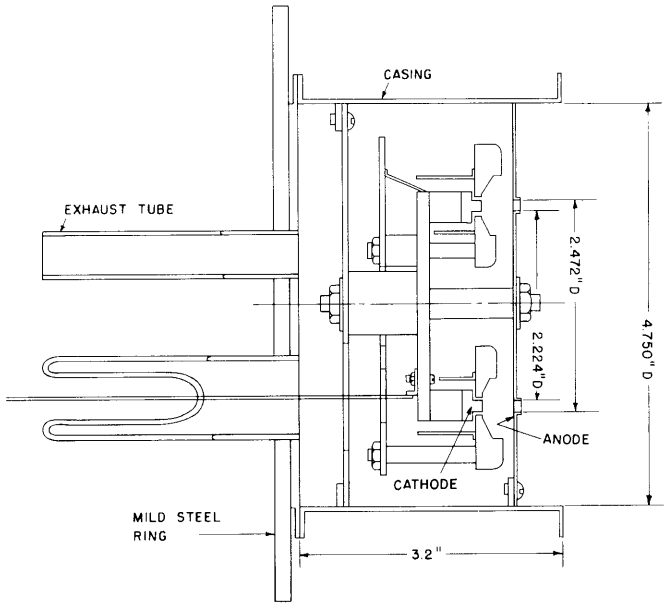

Fig. VI-6. Hollow-beam klystron gun design.

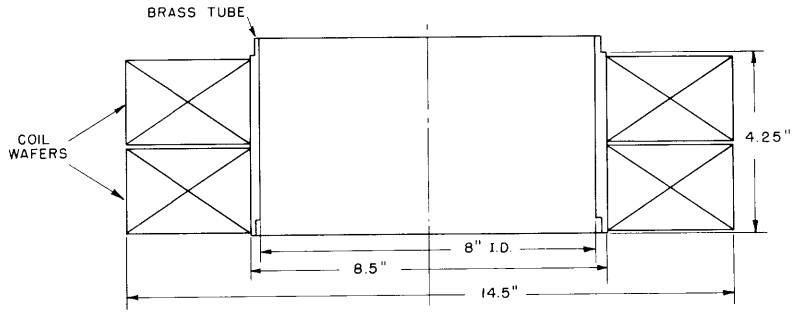

Fig. VI-7. Hollow-beam klystron solenoid coil unit.

3. Focusing Magnet

A seven-cavity klystron is being designed for use with this gun. To maintain the beam in the drift region, a solenoid focusing magnet about 51 inches long is required. The solenoid will have an inside diameter of 8 inches and a minimum flux density of 580 gauss. The preliminary design consists of 12 interlocking coil sections 4.25 inches long. Each section will consist of two coil wafers wound from aluminum tape, 2 inches wide and 10 mills thick, placed between layers of a heat-reactive resin insulating tape, 2 inches wide and 2 mills thick. (See Fig. VI-7.)

The number of amp-turns per coil wafer at a flux density of 580 gauss is approximately 2500. If we chose a current of 10 amp, each coil wafer will have 250 turns of aluminum tape, and a resistance of 0.52 ohm at 100°C.

A. H. Czarapata

4. Low-Q Intermediate Cavities

The high-power multicavity klystron requires that the intermediate cavities have a loaded Q of approximately $Q_L = 25$. This is a much lower Q_L than is normally used in high-power klystron intermediate cavities. In order to obtain such low values of Q_L the cavities can be loaded by additional losses. It was thought that external loading would be too complicated, because 5 coupling lines would have to be brought out of the vacuum and magnet system. Tests were made up on introducing the additional loss into the cavities by spraying the walls with Kanthal. However, only a value of $Q_L = 64$ was obtained.

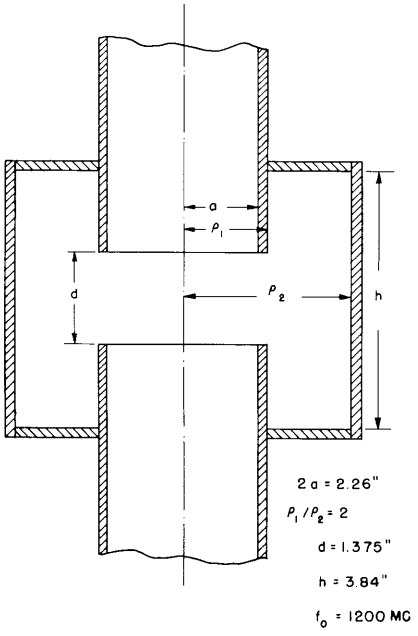

Fig. VI-8. Cavity design.

The loading of a cavity can also be increased by using a larger gap, thereby increasing the electronic loading of the beam. Although the beam-coupling factor M becomes smaller as the gap-transit angle θ increases, it can be shown that the gain-bandwidth product increases until it reaches maximum at $\theta = 2.35$ radians. If we use a gap-transit angle of $\theta = 2.0$ radians and a hollow beam, as outlined in Table VI-I, the loaded Q of the intermediate cavities will be of the order of $Q_L = 20$. If this method is used, it is not necessary to introduce additional loss. The design of the cavity is shown in Fig. VI-8. The R/Q of this design is approximately 140.

H. W. Fock

5. Low-Q Input Cavity

The input cavity must have a loaded Q of approximately one fifth that of the intermediate cavities. Experiments will be made with very tight loop coupling for the input cavity in order to observe the effect on uniformity of field around the interaction gap.

H. W. Fock

E. ELECTRON-STIMULATED ION OSCILLATIONS

It has long been known that an electron drifting through a field-free region emerges with a small modulation that corresponds roughly to the plasma frequency of the positive ions that are trapped in the beam and neutralize its space charge. For ordinary electron current densities, the oscillations are of the order of 1 mc. The rf outputs of klystrons and traveling-wave amplifiers usually display small modulations of the carrier at these frequencies. Cutler (1) and Mihran (2) have summarized some of the experimental observations on magnetically focused beams. Although the magnetic field has a pronounced effect on the oscillations, it is not essential to the process, since reflex klystrons and multigrid space-charge tubes also display this phenomenon.

Pierce (3) analyzed the one-dimensional problem of electrons drifting through stationary ions, and he showed that the propagation constants become complex just below the ion plasma frequency, indicating a potential instability. Since, according to his theory, the instability may be infinite for small signals, it is of interest to see what factors limit the oscillation build-up to finite levels, and what the levels may be. If, for example, as in more conventional oscillators, these plasma oscillations were limited to energies of the order of the primary-beam voltage, ions oscillating with energies of a few thousand volts might be produced.

An experimental and theoretical study of these topics has been undertaken. The theoretical work has been focused mainly on determining the propagation constants of a system that consists of a cylindrical metal drift tube, filled with a plasma of stationary (nondrifting) ions, and a drifting electron beam (Fig. VI-9). Three special cases were studied and the determinantal equations for the propagation constants of

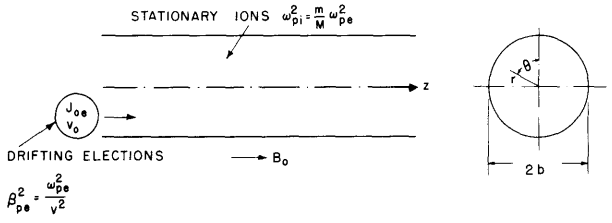

Fig. VI-9. Geometry of waveguide-plasma system.

a TM mode with no angular dependence were found. The wave equation, with $E_z = E_z \exp[j(\omega t - \beta z)]$, is

$$\nabla_T^2 E_z + \psi^2 E_z = 0$$

and if we make $E_z = 0$ at $r = b$, we obtain

$$\psi^2 = T^2 = \frac{m^2}{b^2}$$

where m = root of $J_o(X)$. Then, for ψ^2, we have

1. $B_o = \infty$ (no transverse ion or electron motion)

$$\psi^2 = (k^2 - \beta^2)\left(1 - \frac{\omega_{pi}^2}{\omega^2} - \frac{\beta_{pe}^2}{(\beta_e - \beta)^2}\right) = T^2$$

2. $B_o = \begin{cases} \infty \text{ for electrons} \\ 0 \text{ for ions} \end{cases}$

$$\psi^2 = \left[k^2\left(1 - \frac{\omega_{pi}^2}{\omega^2}\right) - \beta^2\right]\left[1 - \frac{\beta_{pe}^2}{\left(1 - \frac{\omega_{pi}^2}{\omega^2}\right)(\beta_e - \beta)^2}\right] = T^2$$

3. $B_o = 0$

$$\frac{\left[k^2\left(1 - \frac{\omega_{pi}^2}{\omega^2} - \frac{\omega_{pe}^2}{\omega^2}\right) - \beta^2\right]\left[\left(1 - \frac{\omega_{pi}^2}{\omega^2}\right) - \frac{\beta_{pe}^2}{(\beta_e - \beta)^2}\right]}{\left[\left(1 - \frac{\omega_{pi}^2}{\omega^2} - \frac{\omega_{pe}^2}{\omega^2}\right) - \frac{\omega_{pe}^2}{\omega^2}\frac{\beta}{(\beta_e - \beta)}\right]} = T^2$$

A detailed discussion of the roots of these equations will be given in a later report.

The experimental approach is based upon a magnetically focused (or confined) electron beam (Fig. VI-10). Most of our experiments, thus far, have been concerned with looking at oscillations in the collector current (I_c). These were observed on an oscilloscope, but mainly with the aid of a spectrum analyzer. Since the nature of the

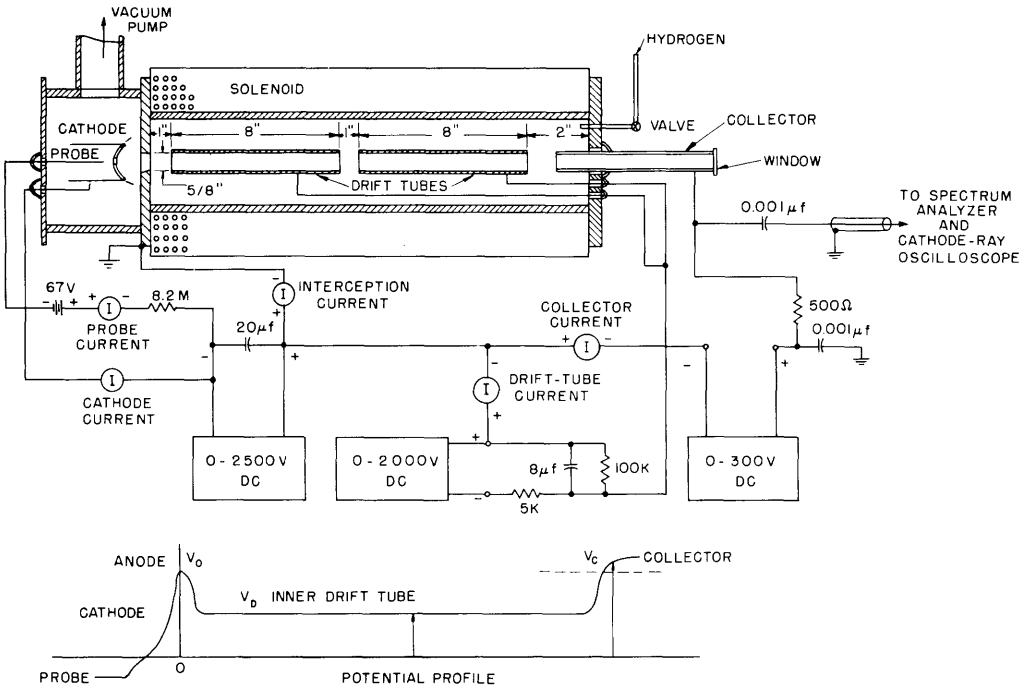

Fig. VI-10. Apparatus for observing ion oscillations in electron beams.

oscillations appears to be greatly modified by secondary electrons, great care was taken in focusing the beam so that the intercepted primary current (not reaching the collector) could be held to approximately 0.1 per cent of the cathode current. Special care was taken to reduce magnet, filament, and plate supply hum. As a result, it is possible to produce highly stable sinusoidal plasma oscillations of 1-5 mc. The potential profile of the system, as shown in Fig. VI-10, indicates that the system will trap ions in the inner drift tube.

Thus far, few quantitative data have been taken, most of the time having gone into setting up measuring apparatus, and getting the entire system to work. Since the magnet can produce only approximately 1000 guass, it is only capable of containing ions of rather low energy. A system with 4000-6000 gauss capability is now being planned, and will be built if the present experiments show further promise.

L. D. Smullin, C. Fried, R. Bevensee

References

1. C. C. Cutler, Spurious modulation of electron beams, Proc. IRE 44, 61-64 (1956).
2. T. G. Mihran, Positive ion oscillations in long electron beams, Trans. IRE, vol. ED-3, no. 3, p. 47 (July 1956).
3. J. R. Pierce, Possible fluctuations in electron streams due to ions, J. Appl. Phys. 19, 231 (1948).

F. HYDROGEN PROCESSING OF STAINLESS STEEL

See "Shop Notes," Section XX, page 170.